Studying defects in periodic structures with Fourier maps

A thesis submitted in partial fulfilment

for the degree of

Master of Science

as a part of the

Integrated Ph. D. programme

(Material Science)

by

Ankush Kumar

Chemistry and Physics of Materials Unit

Jawaharlal Nehru Centre for Advanced Scientific Research

(A Deemed University)

Bangalore, India

March 2013

Dedicated to Nature …

DECLARATION

I hereby declare that the matter described in the thesis entitled **"Studying defects in periodic structures with Fourier maps"** is the result of investigations carried out by me at the Chemistry and Physics of Materials Unit, Jawaharlal Nehru Centre for Advanced Scientific Research, Bangalore, India under the supervision of Prof. G U Kulkarni and that it has not been submitted elsewhere for the award of any degree or diploma.

In keeping with the general practice in reporting scientific observations, due acknowledgement has been made whenever the work described is based on the findings of other investigators. Any omissions that might have occurred due to oversight or error in judgment, is regretted.

_____

Ankush Kumar

CERTIFICATE

I hereby certify that the work described in this thesis **"Studying defects in periodic structures with Fourier maps"** has been carried out by Mr. Ankush Kumar under my supervision at the Chemistry and Physics of Materials Unit, Jawaharlal Nehru Centre for Advanced Scientific Research, Bangalore, India and that it has not been submitted elsewhere for the award of any degree or diploma.

_____

Prof G U Kulkarni

(Research Supervisor)

ACKNOWLEDGEMENT

I am pleased to acknowledge the invaluable guidance and encouragement received from my mentor, Prof. G.U. Kulkarni and for posing this interesting problem. Apart from the thesis work, I am in debt to him for giving me exceptional freedom to work on various exploratory and unconventional problems in this enjoyable and learning year.

I thank my lab-mate Ritu Gupta for fruitful discussions and guidance and Narendra for providing the AFM images of HOPG and feedbacks on thesis.

I acknowledge all my course instructors especially Prof Bala for FORTRAN and Prof Aloknath Chakrabarti for Mathematics.

I acknowledge Department of Science and Technology for funding and JNCASR for facilities (especially library and comp lab staff).

For the enjoyable stay in JNCASR, I am really grateful to my batch mates, lab mates and other friends. I thank my friends for scientific and non-scientific discussions especially Vikas, Sunil, Rukhsan, Dheeraj, Devinder Negi, Rajdeep, Soumik, Kanwar.

Finally, my deep thanks to my mother, father, and sister as well as to my teachers from school and college.

Ankush

PREFACE

Periodic structures play important roles in wide areas of science and technology; however, there are no existing methods to identify and quantify defects in periodic structures. Microscopy examination is costly both in terms of instrumentation and time, and suffer from small field of view. In this study, a method is proposed based on measurable image contrast between periodic lines and the defects within; this is a quantitative Fourier transformation method. A periodic structure under examination is taken as a high resolution image which is then divided into square or rectangular cells. The data within each cell is Fourier transformed and the Fourier intensities of the zeroth and the First order peaks are noted. After applying these procedures to all cells, Fourier maps are produced for the entire image area. The variations in the intensities in the maps (color variables) indicate quantitatively how defective is the image in the cell. Initially, Fourier intensities are compared for various kinds of computer generated defects in periodic pattern as a standardisation procedure. The method is then demonstrated experimentally to quantify defects. Beads spread on a scanner bed served as defects for initial studies. The method was then applied to quantify defects on large area transparent grating electrode as well as on a grating structure produced on graphite (HOPG). The method is extended to periodic biological structures, soldiers in a parade, structural pattern formed of flying birds, oliographic clouds and walking footprints. Once automated, the method can serve analysis of large body of data.

Table of Contents

Studying defects in periodic structures with Fourier maps

1. Introduction

Nature loves symmetry; beauty of periodicity is widely seen around in butterfly wings, moth's eye and honey bee hive etc. [1], giving rise to interesting color patterns, often termed as structural color [2, 3]. Periodic structures in the form of line gratings and meshes play an important role in various applications such as optical gratings, Compact Discs (CDs) and Digital Video Discs (DVDs), microlense arrays, memory bit arrays etc. A periodic structure of a material brings in interesting optical, electrical and other effects and thus a functional property to the structure [4-7]. Optical grating consists of consecutive transparent and opaque line patterns, dispersing light into different colours (wavelengths). Diffraction gratings are extensively used in spectroscopic tools, imaging, optical communications, networking and data storage. CDs and DVDs consist of pits in a spiral groove from centre to the edge (which appears like a set of parallel lines in small area for storing data). A functional material in pattern can serve as a sensor as well. For example, a hydrogen sensor developed in our laboratory [8] employed Pd line gratings (periodicity ~ 1.5μm), wherein topographical changes in the grating due to hydride formation led to measurable variations in the diffraction efficiency. Periodic structures of dielectric materials are extensively used in photonic crystals controlling light propagation [9, 10].Optical gratings made of plasmonic materials have gained importance in the form of antennas as they can be used to spatially confine the electromagnetic field [11]. Such structures in micro and nano-scale are made by self-assembly of various building blocks, an example being polystyrene beads [9, 12-15]. Other examples of periodic structures include micro lens arrays as light concentrator for solar applications [16-18], DNA chips etc [19-21]; the latter is a collection of microscopic DNA spots on solid substrate used for investigating gene expressions.

These periodic structures are fabricated by multiple steps in lithographic processes sometimes involving self-assembly [22, 23]. Due to many unknown and uncontrollable parameters, the fabrication may bring in uneven broadening, diffusion and many unavoidable defects. The process of self assembly suffers from problems of dislocations at the grain boundary [9, 12, 13, 24]. However, in all the above structures, periodicity of the material in pattern is of utmost importance. Any deviation would result in degradation or malfunctioning of the device. A quality of the periodic structure is currently examined by suitable microscopy techniques depending on dimension of periodicity and resolution required. Currently used techniques are optical microscope, confocal microscope, scanning electron microscope; a faster technique for large area applications is optical profilometry [25-27], based on interference from reflected light from sample and the reference. Similar methods based on interference and reflections are also reported in literature [28-33]. All these methods are costly both in terms of instrumentation and time, and suffer from small field of view. Comparing two local regions on a given sample substrate, even if closer they are, is not so straightforward. Thus, the present techniques are nearly unfeasible for quality check of large area patterns extending into several millimetres to centimetres.

2. Scope of Investigation

To overcome the limitations of the present methods for routine but quantitative evaluation of periodic patterns, here a method is proposed which makes use of a scanned image of the periodic structure under examination, in a 2D Fourier analysis having defined cells or domains covering the entire area of the periodic structure. The variations in the Fourier peak intensities would stand for the sample deformities. The method is extendable to non-periodic patterns or even plain surfaces, by simply overlapping a calibration grating on top while scanning (by a suitable method).

A similar method based on optical diffraction has been developed in our laboratory [34]; in this method ,the sample under investigation (a metal nanowire grating structure) was scanned with a pointed laser beam and from each region (pixel), diffraction data was obtained, the diffraction efficiency was calculated. These values were displayed in the form of a $n \times n$ pixel map which clearly brought out defects in the periodic structure present in different pixels. While this method has numerous advantages over microscopy or absorption measurements, and is specifically applicable for studying variations in complex refractive index value, it is quite cumbersome if it is to be applied to routine examination of a large area filled with periodic structures. The method presented in this work rules out the shortcomings of methods of literature. The method can be applied to images of all orders; atomic images to camera images.

3. Methodology

The investigation involves intentionally creating the defective surfaces, overlapping the defective site over a standard periodic pattern and quantifying its effect on Fourier transformation. In the thesis, 'defect' is very generic word used for any blot, scratch, impurity, bulging etc which shows different contrast as compare to periodic lines in an image. The defects can be of any shape and size. The length scale of defects plays an important role. Some of the defects can be easily visualized with the naked eyes and may not require any analysis by Fourier transformation. When the length scale of defects is beyond the resolving power of eyes, it is when that this technique becomes more effective. The basic requirement of this method is that the periodicity of the grating should be of the same order as the size of defects. The present study is carried out in two ways:

i) Computer generated images of gratings and defects; the latter with varied position, shape and size with respect to the grating pattern. This step authenticated the code and the procedure for extending to experimental analysis.

ii) Experimental analysis using a standard grating and introducing known defects while scanning under a scanner bed. The method is then extended to 'real' samples such as electrode array.

Fourier transformation is one of most widely used transformation in Physics. Kernel for Fourier transformation is $\frac{e^{-iKx}}{\sqrt{2\pi}}$ and limits as $-\infty$ to ∞. Necessary and sufficient condition of Fourier transformation are known as Dirichlet's conditions which are:

Function should be square integrable, single valued, piecewise continues and should have upper and lower bounds [35, 36].

Fourier Theory is a mathematical method proposed by Joseph Fourier (1760 -1830) to express any periodic or non-periodic function into sum of series of sinusoidal terms of various wavelength, which are sub integral multiple of λ. It was highly opposed by mathematicians of those days including Lagrange. The scope of Fourier transformation is very wide. Now it is widely used in optics, spectroscopy, acoustics and electrical signal analysis etc. It is also used in condensed matter physics while dealing with reciprocal lattice. Physically saying Fourier transformation is the calculation and operation required to see frequency domain of signal. In dynamic experiments, time is the abscissa and amplitude, the ordinate. Fourier transformation is a transformation by which one can express the signal into frequency as abscissa and amplitude as the ordinate.

Fourier transformation in its usual form is,

$$F(\nu) = \int_{-\infty}^{\infty} f(t)\, e^{-2\pi i \nu t}\, dt \qquad (1)$$

Data processing involves discrete data sets and not continuous functions! To perform the Fourier transformation of discrete numbers, one uses discrete Fourier transformation. Let f(x) is continues function with finite N samples, denoted as f (0), f (1), f (2) …..f (N-1).

Since intergradient exists only at sample points thus Fourier transformation in discrete form is

$$F(\nu) = \int_{0}^{(N-1)T} f(t) \frac{e^{-2\pi i n \nu}}{N}\, dt \qquad (2)$$

$$= \sum_{n=0}^{(N-1)} f_n \frac{-2\pi i \nu n}{N} \qquad (3)$$

Fourier transformation can be generalized to multi dimensions also. For two dimensional Fourier transformation is given by:

$$F(K_x,K_y) = \iint_{-\infty}^{+\infty} f(x,y)\, e^{2\pi i\,(k_x x + k_y y)}\ dx\ dy \qquad (4)$$

It involves first taking Fourier transformation of row followed by Fourier transformation of column.

Fourier transformation calculation can be quite intensive depending on the size of the data set. In order to efficiently calculate FT, an algorithm commonly known as Fast Fourier transformation, was firstly discussed by Cooley and Tookey in 1965 [37] although its origin can be traced to Gauss. It reduces number of computational steps from $2N^2$ to 2N log N which can have effect for large N. It is a divide and conquer algorithm based on the idea of recursively breaking down any composite $N = N_1 N_2$ into N_1 and N_2.

3.1. Computer generated images

An image is a 3D mathematical array where x and y coordinates represent position in terms of pixels, while the 3rd coordinate represents intensity. Intensity is expressed in the form of greyscale ranging from 0 to 255 where 0 represents black and 255 represents white. Mathematical arrays for designing an image are obtained using MATLAB or FORTRAN programming. To assign a defect in the designed image, the intensity value at specified coordinates was allotted manually. Grating and defect images generated separately are overlapped computationally as shown in flow chart (see **Figure 1**). For the purpose of computation, the overlapped image was divided into m × m cells following which 2D Fourier transformation of individual cells was performed. From the Fourier image, the locations of the zeroth and first order peaks and their corresponding intensity values were identified. The spacing in reciprocal space was normalized in such a way that each unit in the Fourier plot represented 1 pixel inverse. Thus, if the real image has a periodicity of 50 pixels then in FFT plot, the first order maxima would appear at 1/5 unit inverse = 0.02 units inverse.

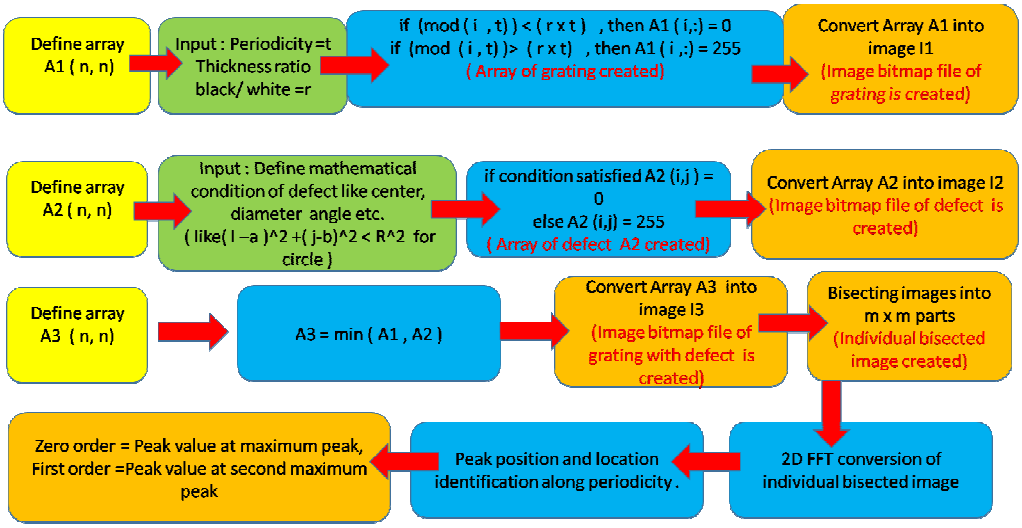

Figure 1. Flow chart of programming to create the grating, defects and the overlapped image; followed by2D Fourier transformation.

3.2. Scanned experimental images:

Standard gratings were drawn in Adobe illustrator (Version : CS) with equal black and white line spacing resulting in a periodicity of ~2 mm covering a square region of 20 cm × 20 cm. The image was transferred to a photo paper as shown in **Figure 2** with a photo printer (HP Photosmart 7550) at 1200 dpi (equivalent of 21μm) resolution.

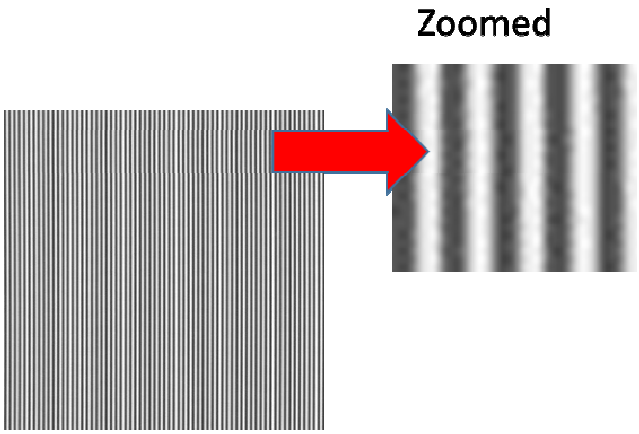

Figure 2. Printed grating pattern with periodicity of ~ 2 mm and size 20×20 cm^2

Thus, printed standard grating was scanned at 800 dpi (equivalent of 32 μm) resolution. The grating itself can be a sample for analysis wherein the defects produced printing may be analysed. Having analysed the grating in detail and certified, other sample surfaces may be overlapped while scanning and the 'overlapped' image may be analysed for defects in the sample. As an example of the defect, glass beads (~2 mm size) spread over a scanner bed overlapped with the standard grating can be used for demonstration. A scanned image of standard grating and the overlapped image of standard grating and beads is cropped with gimp image editor or for bulk cropping with Image magick terminal commands (LINUX OS) in a form of square cell. The number of divisions of image was chosen such that divided images are similar. FT analysis of divided image was done similar to computational images.

4. Results and Discussions

4.1 Analysis for computer generated defects

4.1.1. A periodically patterned image

The diffraction pattern observed from an optical grating, also known as Fraunhofer's diffraction, is essentially Fourier transform. This is illustrated computationally below. Grating consists of alternative opaque and tranparent lines represented as black and white line in our figures. Fourier transformation of a 2D line grating of periodicity, is represented by points in Fourier space positioned at +1/a.

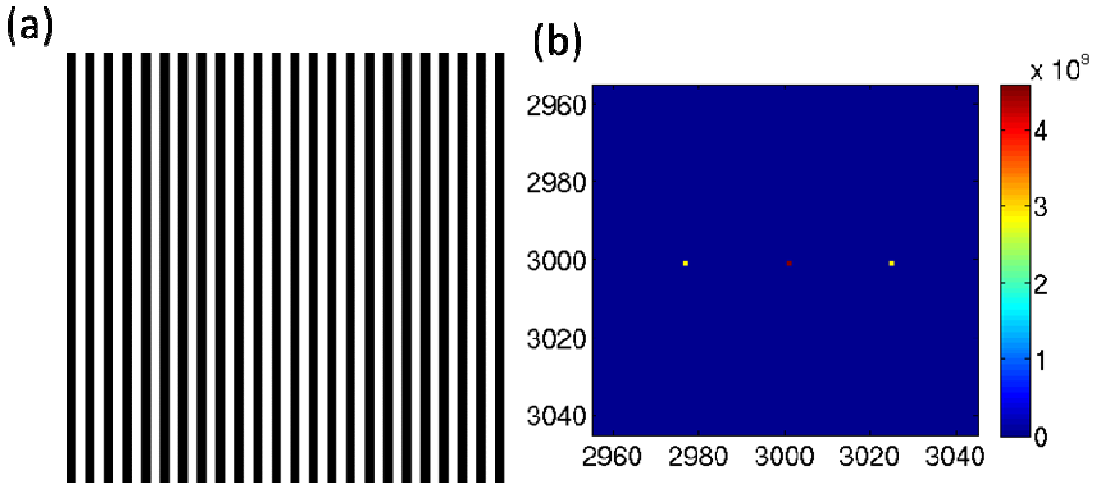

Figure 3. (a) Computer generated Image of grating pattern of 6000 × 6000 pixels. (b) Zoom in view Fourier transformed image of 6000 × 6000 pixels of the corresponding grating pattern

For example, a test grating pattern generated in computer is shown in **Figure 3a**. The zoom in view of the Fourier map for the corresponding image is depicted in Figure 3b. As seen clearly, distinct and sharp spots are obtained on performing Fourier transformation of the above image. The color scale on the left shows the intensity of Fourier spots obtained. The high intensity spots in red and yellow correspond to the zeroth and first order peaks respectively.

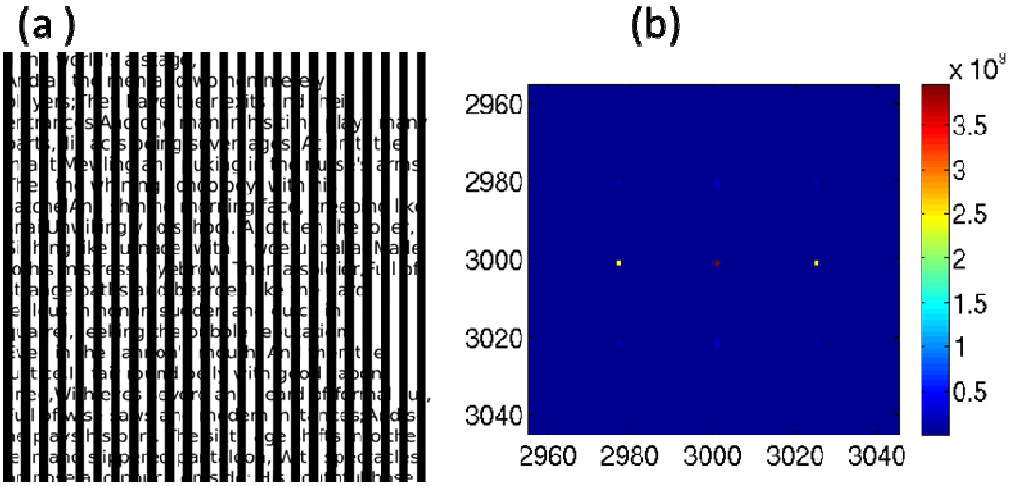

Figure 4. (a) Computer generated grating image (6000 × 6000 pixels) with the defects of random alphabets (b) Zoomed Fourier image of the corresponding image

Figure 4a represents Fourier image of the defective grating. Here, the standard grating is seen with some writing in the background, the latter representing defects. The positions of peaks are unaffected but the peak intensity of zeroth as well as of the first order peaks are reduced due to the defective grating.

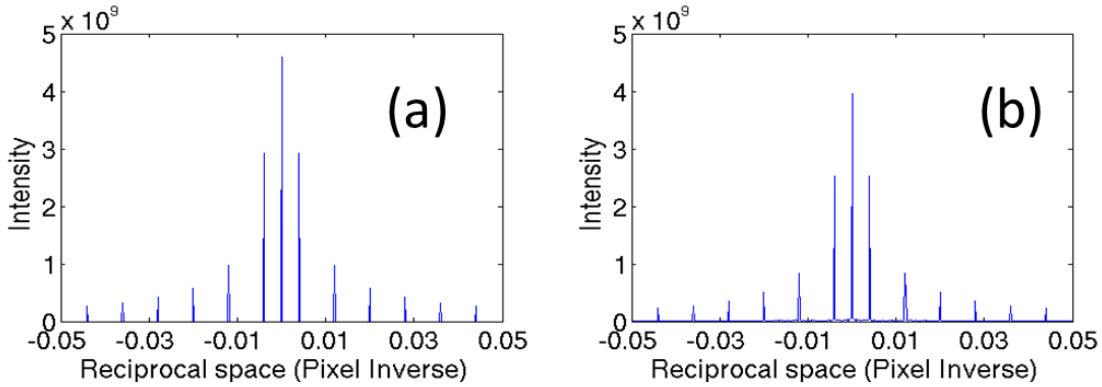

Figure 5. Comparison of Fourier peak intensities for (a) standard grating with (b) grating overlapped with text (Figure 4a). Central peak represents zeroth order whereas the peaks adjacent on either side represent the first order. Other peaks are of high order.

The quantitative comparison is shown in **Figure 5**, which represents intensity distribution along direction of periodicity (X axis). The peak positions are unaffected with the defective grating; whereas the peak intensities are diminished.

To understand effect of defects on Fourier image, it is necessary to perform quantitative variation in Fourier intensity with size. Few terms are defined for convenience:

$$\text{Relative Intensity change of zeroth order, } R_z = \frac{(I_S^Z - I_D^Z)\ x\ 100}{I_S^Z} \quad (5)$$

$$\text{Relative Intensity change of first order, } R_F = \frac{(I_S^F - I_D^F)\ x\ 100}{I_S^F} \quad (6)$$

where, I_S^Z represents the zeroth order intensity of the standard grating

I_D^Z, represents the zeroth order intensity of the defective grating

I_S^F, represents the first order intensity of the standard grating

I_D^F, represents the first order intensity of the defective grating

These terms are used in the following sections.

4.1.2. Effect of size of a circular defect

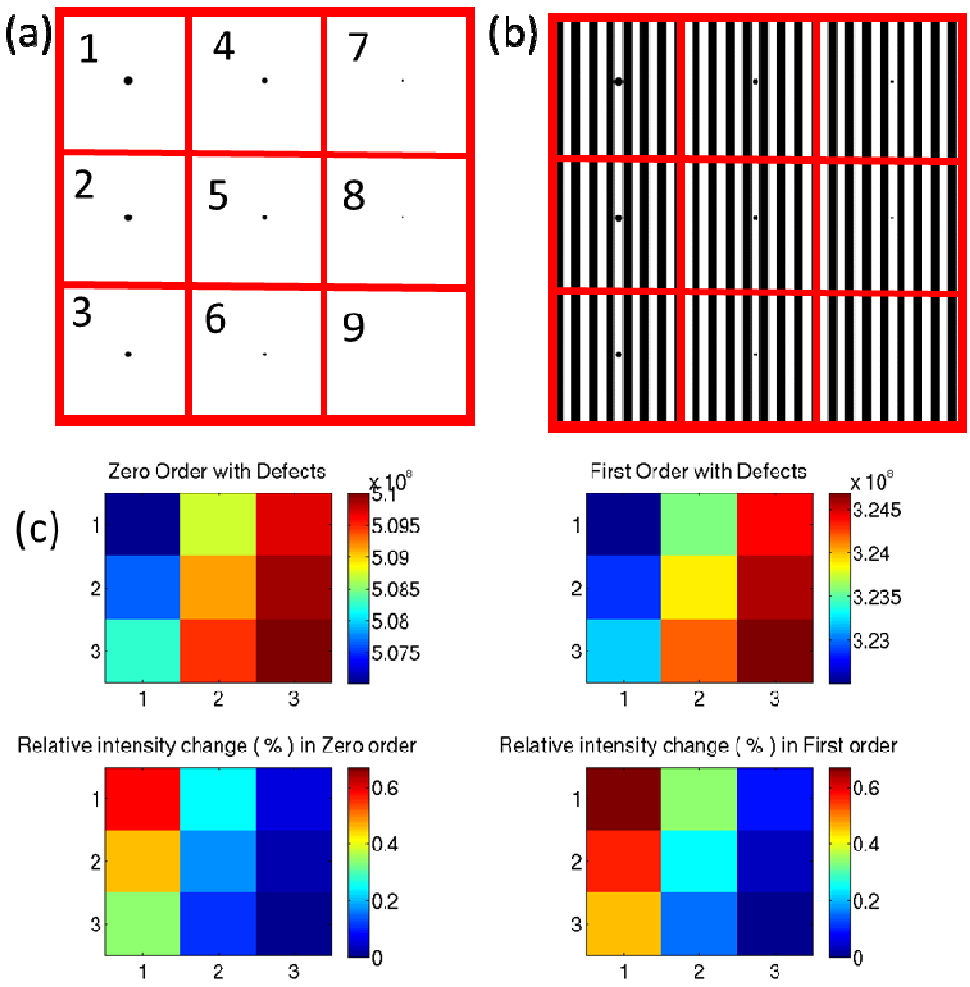

Figure 6. Effect of variation of zeroth order and first order intensities with defect (a) circular defects with decreasing size in different cells (b) defects overlaid with grating (c) Intensity maps for zeroth order and first order peaks. Relative intensity variations have been calculated after substracting corresponding intensities of the standard grating.

Figure 6a shows an image of 6000 pixels with defects represented by dark circles of decreasing size in subsequent cells. Defect diameters in cell number 1 to 9 are 120, 108, 94, 80, 66, 52, 38, 24, 0 pixels, respectively. In Figure 6b, the defects are seen overlaid with a standard grating of periodicity 250 pixels. The intensities of the Fourier peaks are found to decrease with the defect size as shown in Figure 6c.

4.1.3. Effect of position of a circular defect

In the images discussed above, the defects have been located to be midway between two dark lines (in white region), but in a practical situation, the defect can be anywhere.

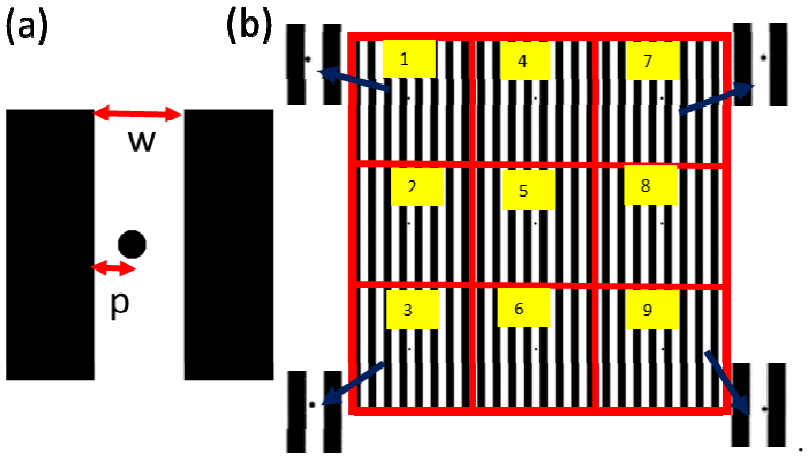

Figure 7. (a) Position distance of circular defect and thickness of white line (b) Image of defect of diameter pixels at different positions. Zoomed images are also shown.

Figure 7a shows an image in which a circle representing defect is shown at one of different locations within the white stripe (region).The distance of the defect from the edge is denoted by p, which moves to the right in subsequent cells. In the shown image (Figure 7b), there are 6000 pixels with periodicity of lines being 250 pixels and the defect circle, 40 pixels.

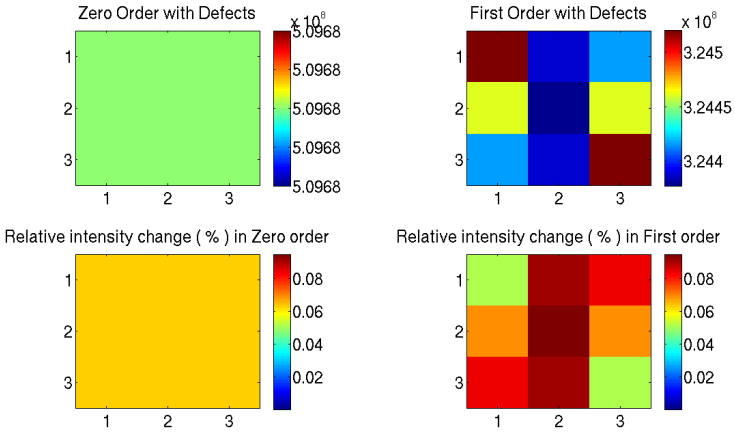

Figure 8. Fourier intensity maps of zeroth and first order peaks (top) along with relative change in zeroth and first order intensities (bottom). These maps correspond to Figure 7b.

Fourier transformation of each cell is evaluated and corresponding zeroth order and first order are plotted in **Figure 8**. It is clear from the figure that the zeroth order (maps on the right) shows the same value whereas the first order shows significant variations with respect to the position of the defect. It is interesting to note that the change in the intensity is maximum when the defect is in the center of the white region and falls off on either side (see **Figure 9**).

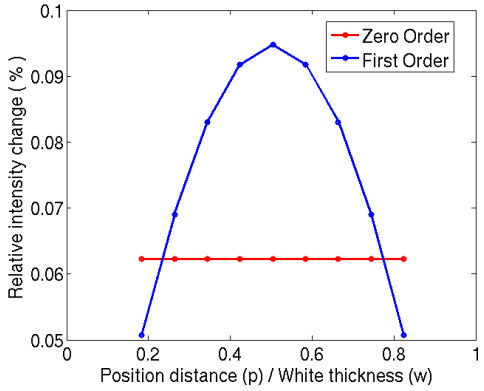

Figure 9. The relative changes in the intensities shown with respect to relative position (p) of the defect divided by grating white thickness (w).

Relative variation in the zeroth order peak is independent of orientation, as expected.

4.1.4. Effect of orientation of a defect

All defects may not be of same shape; a small irregularity in shape can bring in orientation effects. To study this aspect, elliptical objects with major axis 100 pixels and minor axis 50 pixels were chosen to represent defects. Fourier transformation of defect overlapped grating image was carried out.

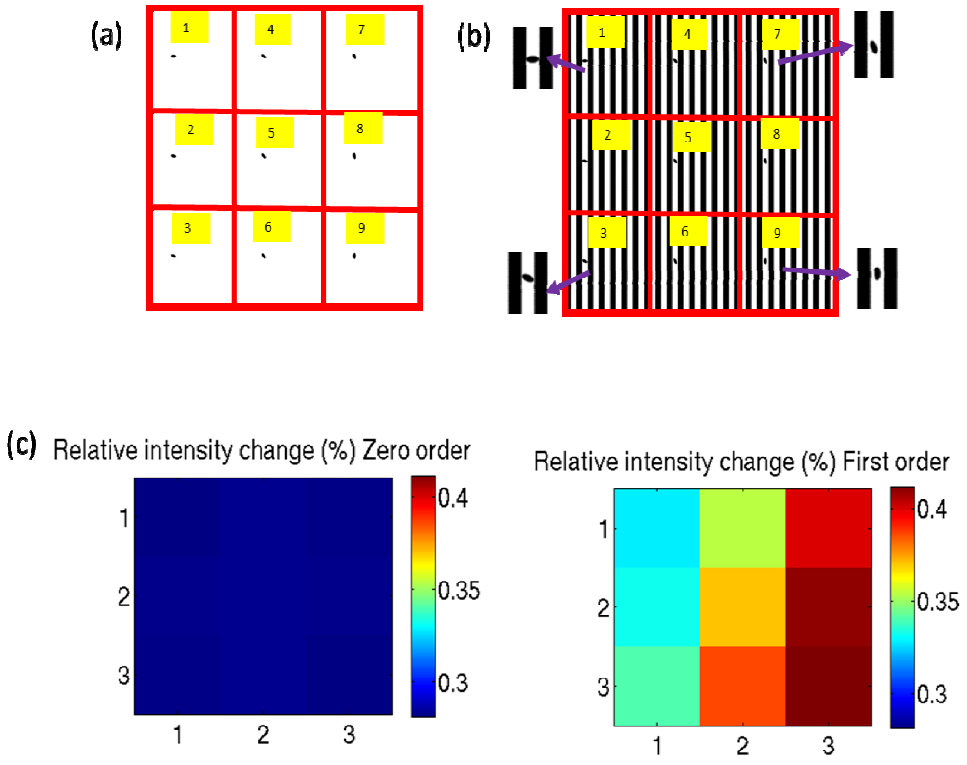

Figure 10. (a) Defect represented by ellipse is rotated by 11.25 degrees in subsequent cells (b) Elliptical defects overlapped by grating (c) Relative intensity change of zeroth order and first order peaks.

As shown in **Figure 10a** in the first cell, the elliptical defect has its major axis perpendicular to the grating periodicity; in the subsequent cells, the defect is rotated 11.25 degrees clockwise such that in the 9th (last) cell, its major axis became parallel to the grating periodicity. Figure 10b contains the grating with 6000 pixels and periodicity of 250 pixels (periodicity > ellipse size) is seen overlapped with the defects. It is clear from Figure 10c that the zeroth order peaks from different cells are hardly affected by the

rotation of elliptical defect whereas interestingly, the first order peak intensity shows the orientation effect. The intensity is higher when the major axis is parallel to the grating periodicity and minimum in case when it is perpendicular to periodicity.

4.1.5. Effect of non-straight line of grating

An optical grating or any periodic pattern may have a possible defect of few non straight lines. To study this aspect, relative variation in Fourier intensities were calculated for a grating with few slightly tilted lines.

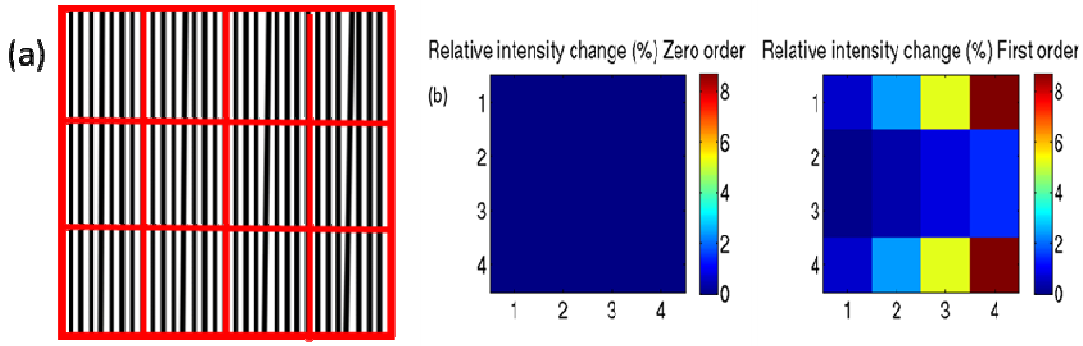

Figure 11. Effect of non-straight lines: out of the eight lines in each cell, the central line is tilted to i) 0.25, 0.5, 0.75and 1.00˚ respectively. a) Image of the defected grating, Relative intensity changes in b) zeroth order and first order intensities.

Grating with few non straight lines are shown in **Figure 11a**. In this defective grating having 32 lines divided into 4x4 cells, the 4^{th}, 12^{th}, 20^{th} and 28^{th} lines (middle line of each cell) are rotated by 0.25, 0.5, 0.75and 1.00˚ respectively. As shown clearly in Figure 11b, the zeroth order intensity is hardly changed but the first order intensity shows very high relative variation (it is 8% for just 1˚ rotation). Hence in quality checking of straight lines of grating, the zeroth order intensity is completely insensitive whereas the first order intensity is highly sensitive.

4.1.6. Grating phase problem and its possible solution

The effect of defect size on the Fourier intensities is discussed, when the defect was lying in the middle of the grating lines. However, one may consider a more complicated situation where the defect can be randomly distributed. Here, defect circles can be masked completely by black area, partially by black area or may not be even masked depending how grating is placed with respect to the defect(s). Assuming the initial position of the grating to have phase zero, the grating is displaced by a fraction of the periodicity, which may be termed as 'initial phase'. Different scenarios depicting defects overlapped with gratings of different phases are shown in **Figure 12**.

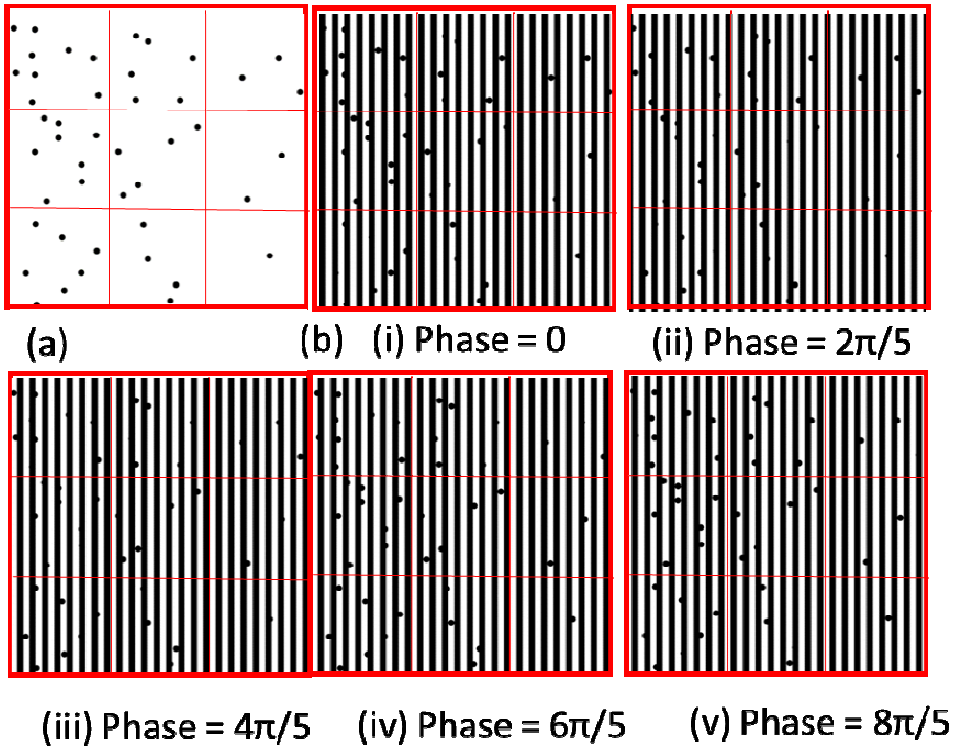

Figure 12. (a) Random circle defects with number of defects in subsequent cells are from 9 to 1. (b) standard grating with different initial phase is overlapped with the defects

As shown clearly, different initial phases of the grating lead to different overlapped images and thus, the masking of a defect depends on the phase of grating.

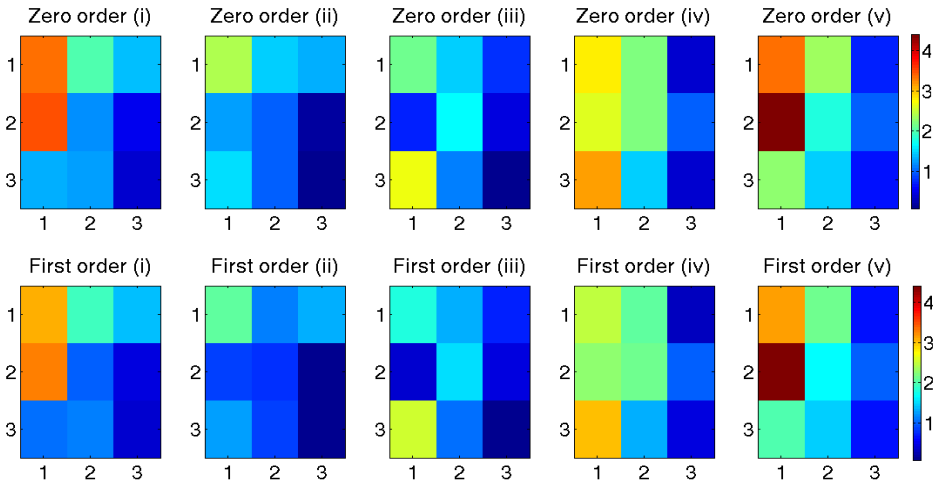

Figure 13. (a) Variation of zeroth order and first order of images of Figure 9 (i to v).

Figure 13 shows the Fourier intensity map for the images discussed above. It is clear that different gratings positioned differently lead to different zeroth and the first order intensities, and will not represent the true scenario. If in a cell, more defects are seen in the white region, the relative variations in the intensities are more pronounced while if defects are overlapped on the black lines, the variations are rather less. This huge variation in the intensity due to positioning of the grating can be misleading an observation. The reason for this inconsistency is that the defect masked by the black area does not contribute to the response (in Fourier transformation). In order to circumvent this problem, one needs to use gratings with varying phases overlapped with the defects and estimate the mean values of the Fourier intensities.

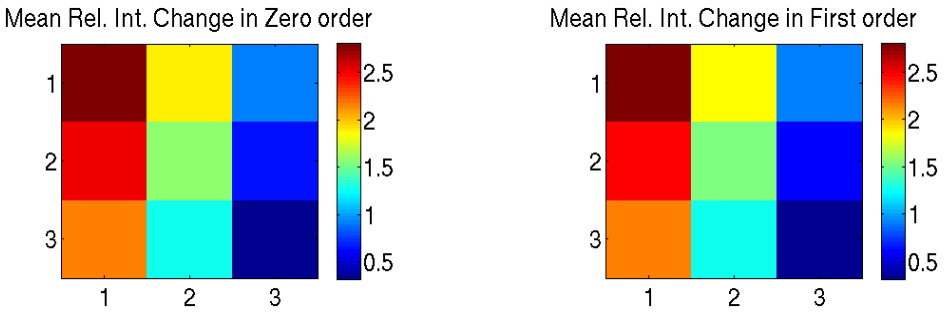

Figure 14. Mean values of zeroth order and first order intensities for 5 different phase gratings mentioned above.

It is clear from **Figure 14** that the mean values for various initial phase grating are in agreement with the number of beads.

4.1.7. Comparison of black and white defects

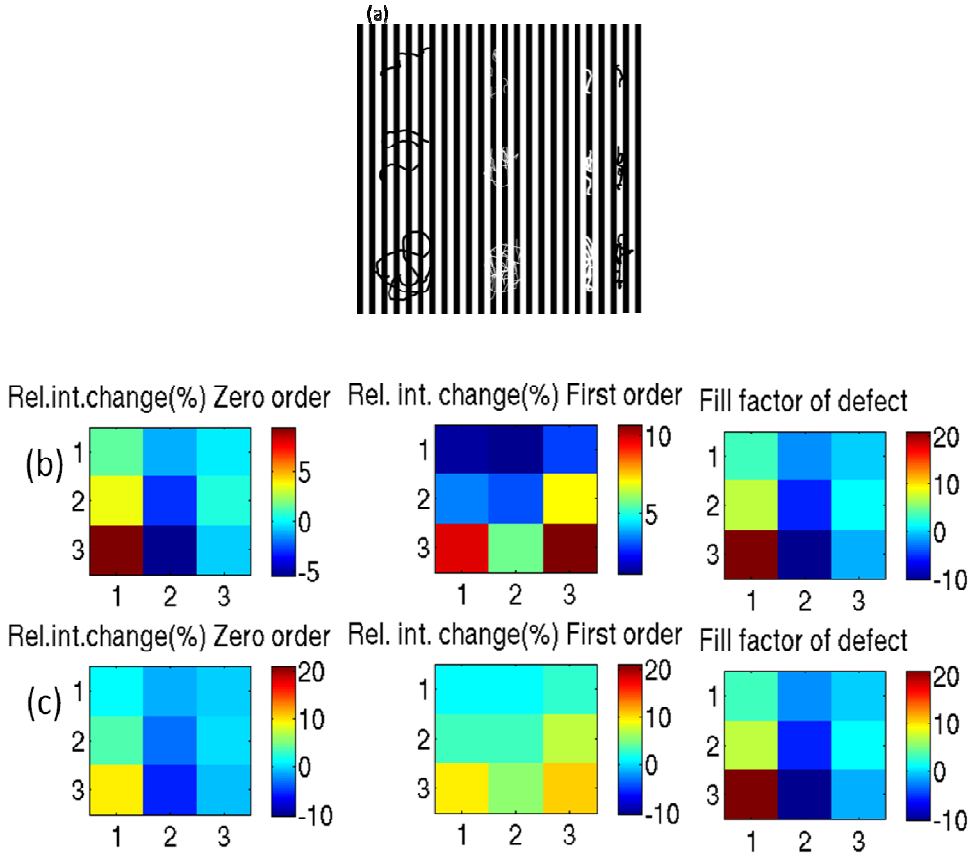

Figure 15. (a) Image showing arbitrary scratch defects on grating. On the right side, there are black defects, white defects in the middle region and white and black defects on the left. (b) Relative changes in zeroth and first order intensities along with the fill factor of defect, (c) Maps with same common scale.

Grating consists of alternative opaque and tranparent lines represented as black and white line in the figures presented in this work. Defects can be of two kinds, namely, non-ideal opaque (black) part and non-ideal transparent (white) part. as shown in **Figure 15a**.

Figure 15b shows the corresponding relative variation in zeroth order and first order intensities. The fill factor, defined as area of the total black region (grating + defect) divided by total cell area is also shown for comparison.

As seen in the figure, the defect size increases down the column. As shown clearly, for black defects, the zeroth order and the first order intensities as well as the fill factor all decrease with the defect size. For white defects on the other hand, the zeroth order intensity increases while the first order intensity and the fill factor decrease. In the left region where both black and white defects are present, interestingly, the zeroth order intensity and the fill factor remain nearly unchanged while the first order intensity shows a noticeable change. Thus, only the first order intensity (the Fourier transform) is alone sensitive to detect and quantify all kinds of defects. This observation is important as in practical situations such as optical gratings and lithographic patterns; defects of different kinds may be simultaneously present.

4.2. Analysis from experimental scanned data

4.2.1. Quantification of beads

Computational defects and their variations in the zeroth and the first order intensities are discussed in the above section. The discussion henceforth is pertaining to experimental observations. **Figure 16** presents a scenario by using scanned images of a grating and the grating with defects. Here, the defects, represented by commercially available black ornamental beads with diameter of ~ 3 mm, are overlapped with a standard printed grating with periodicity of ~ 2 mm.

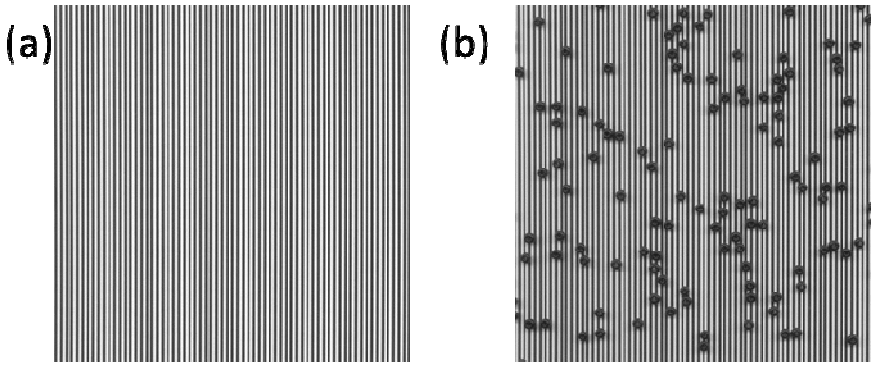

Figure 16. (a) Scanned image of the standard grating (b) the scanned image of beads overlapped with the standard grating

Initially, a computer generated standard grating was printed on white paper with a periodicity of ~ 2 mm which was scanned to produce an image shown in Figure 16a (for details, see methodology, section 3.2). Scanning was done 10 times to examine any intrinsic errors in the scanner process. The scanned image was then divided into 8x8 cells. Fourier intensities for individual cells are shown in **Figure 17.**

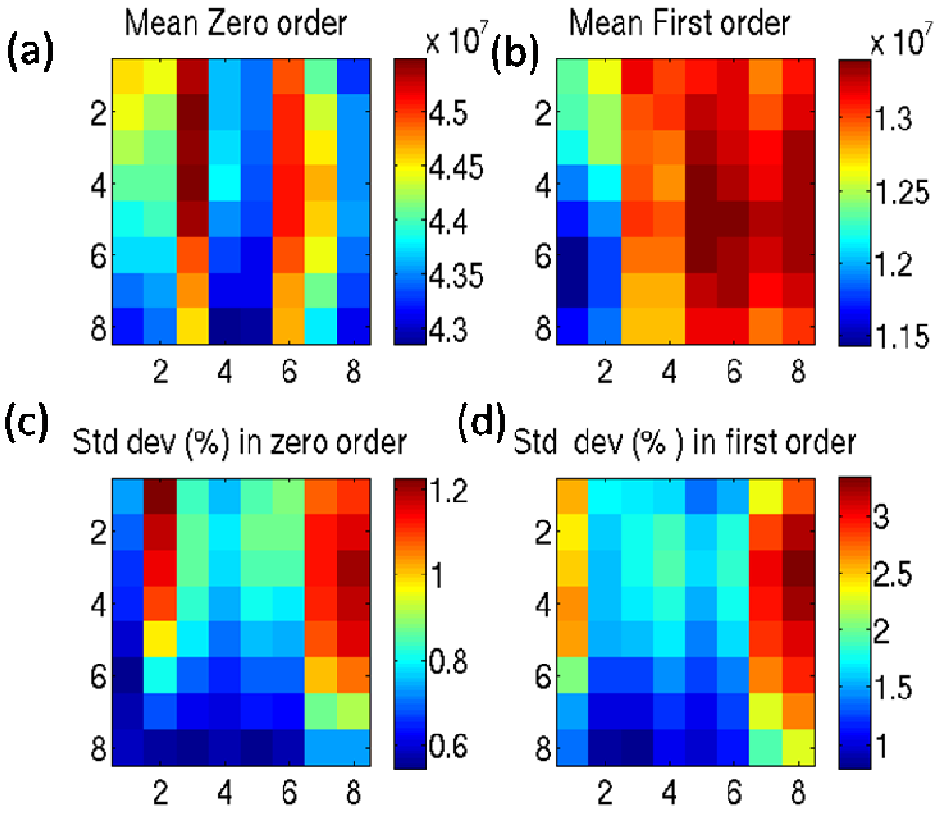

Figure 17. Analysis of 10 measurements of the standard grating (a) Mean zeroth order intensity (b) Mean first order intensity (c) Standard deviation in zeroth order intensity (d) Standard deviation in first of order intensity

Figure 17 shows the mean and standard deviation values for zeroth order and first order intensities for the 10 scans of the standard grating. During this measurement, the scanner cover was intentionally opened and closed for each scan so that any possible variation, temporal and positional, became part of the error, as would be the case in realistic situations. Interestingly, the standard deviation in the zeroth order intensity (error bar for zeroth order) is less than 1.2% while that of the first order (error bar of the first order) is less than 3%. This experiment sets the upper limits for errors in defect detection.

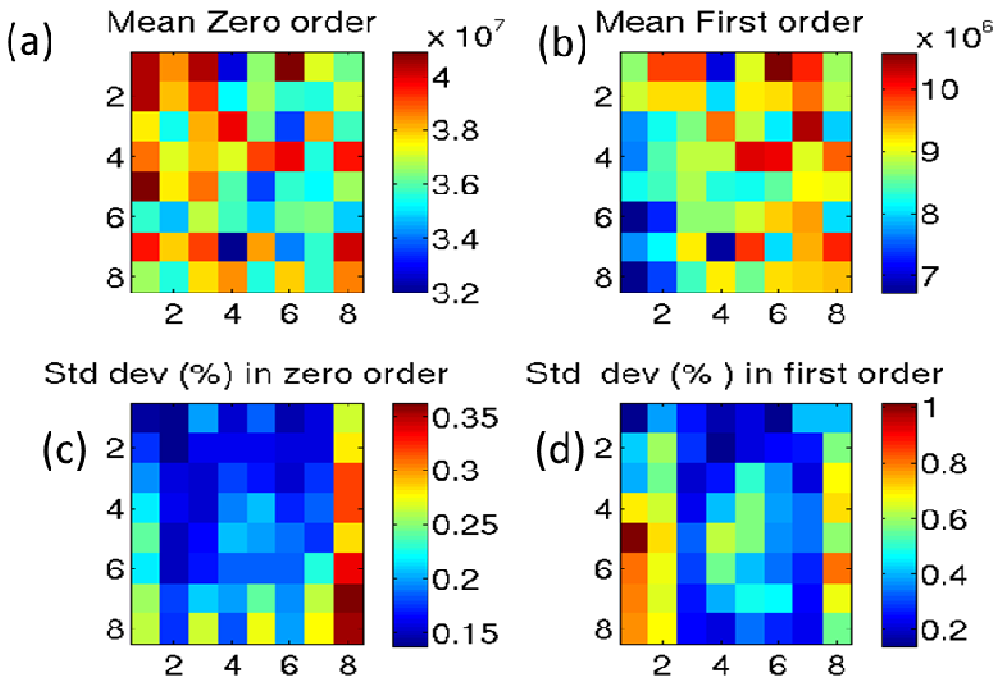

Figure 18. Analysis of 10 measurements of grating placed on beads (a) Mean zeroth order and (b) Mean first order intensities (c) Standard deviation in zeroth order intensity (d) Standard deviation in first order intensity.

In the subsequent step, the beads were spread over the scanner bed and the grating is placed over it. To avoid possible displacements of beads, the scans were done without opening the cover. One such scanned image is shown in Figure 16b. **Figure 18** shows the mean and standard variation for the zeroth order and the first order intensities of individual cells for the 10 measurements. The areas with more beads are showing less Fourier intensities, represented with blue color while areas with no beads are brown, (higher Fourier intensities). **Figure 19** compares relative variation in Fourier intensities with actual number of beads in individual cells.

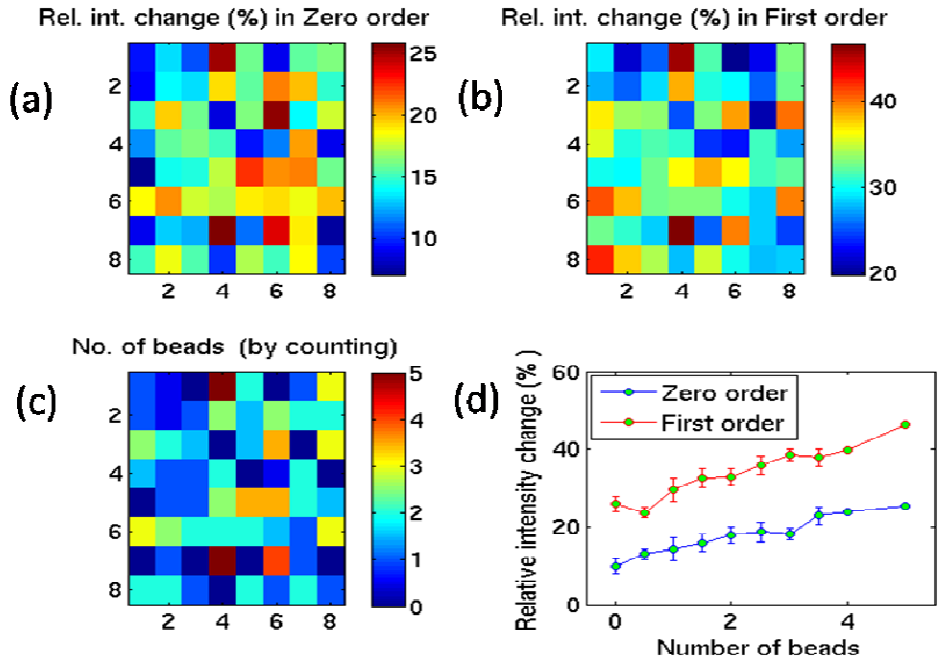

Figure 19. (a) Relative change in zeroth order intensity (b) Relative change in first order intensity (c) No of beads in the cell by counting (×d) Relative intensities change with number of beads

Figures 19a and 19b shows the relative variation in the zeroth and the first order intensities of the individual cell while Figure 19c shows actual number of beads per cell by manually counting beads present in each cell. On comparing Fourier intensities and actual number of beads, it is clear that the intensities indeed represent the number of beads; the colour maps of number of beads are similar to Fourier maps. A more quantitative analysis is shown in Figure 19d, where the Fourier intensities are seen to increase with the number of beads. The low values of the standard deviations in Fourier intensities (1.2% and 3%, for zeroth and first order respectively) bring confidence in the measurement. The present measurements are performed at just 800 dpi with the aged scanner. This above experiment and analysis is essentially a proof of the idea, which can be easily extended to defects of much smaller sizes using high resolution scanner as well as standard grating.

4.2.2. Periodicity of Ag lines

Ag electrodes are highly useful as transparent conductors [38]. These electrodes can be made by thermal evaporation through micro structured shadow masks, photolithography, screen printing, inkjet printing etc. In spite of all careful designing and printing steps there is always a probability to encounter the defective areas while fabricating grids over large areas. **Figure 20** shows one of Ag transparent conductor fabricated in our laboratory by Ag ink patterning. The black regions in Figure 17 represent Ag lines, whereas the white (grey) area is the PET substrate. Such electrodes are expected to be uniform over large areas for reliable functioning in various optoelectronic devices. In the present case, the given structure offers various non-uniformities over the large area (~8 × 8 cm^2), ideally suited to demonstrate the developed method. Thus, to locate a good periodic area of the electrode and to mark a defective area is very important quality check in lab experiments as well as in industries. Possible defects in this case are diffused or rubbed ink which can affect electrical properties to a great extent.

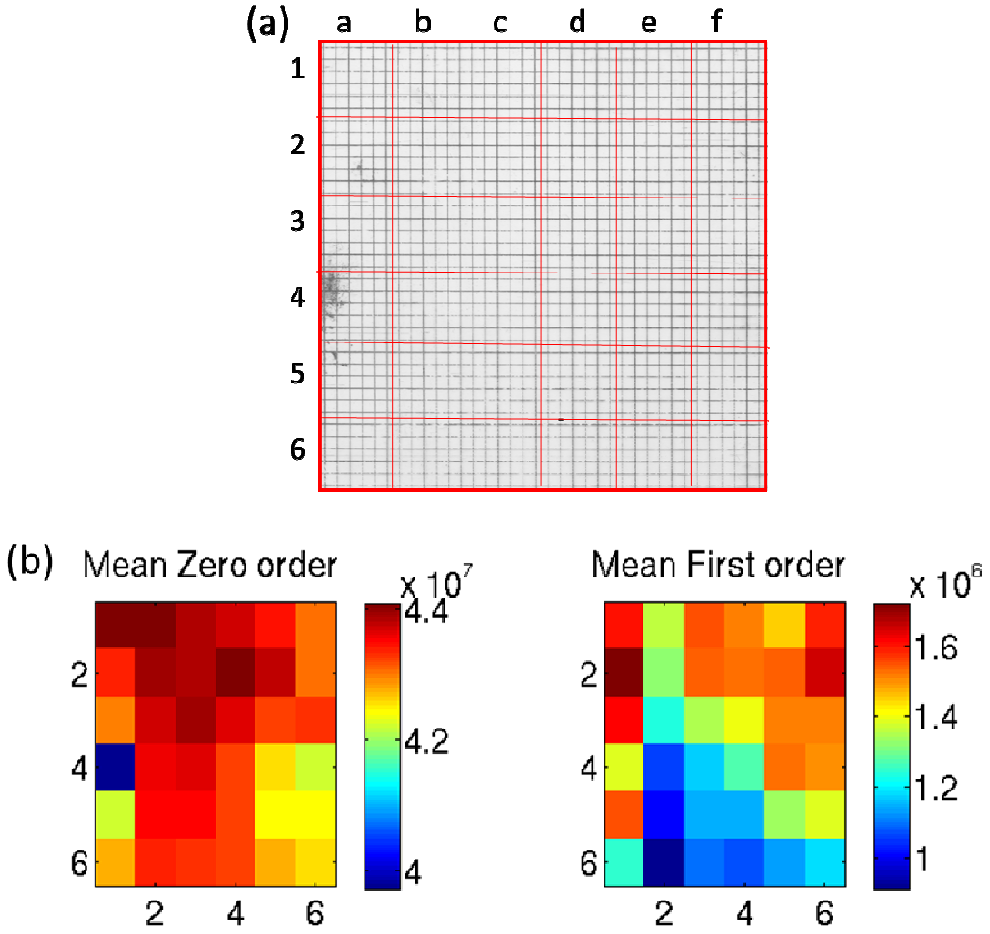

Figure 20. (a) Scanned image of a (cells shown with red grid) Ag electrode (b) zeroth and first order intensities of scanned pattern of Ag electrode

The scanned image of the electrode was divided into 8x8 cells (cells shown with red grid). Fourier transformation of individual image cell was taken. Figure 20b represents the zeroth and the first order intensities of the individual cell. As shown, 4a cell exhibits diffused ink and interestingly, the corresponding zeroth order intensity is reduced abruptly. In cell 5b and 6c, Ag lines are somewhat discontinuous; the first order intensity is reduced at those cells. Thus, cells with discontinuous lines show that less value of the first order intensity while cells where Ag ink is diffused, exhibit less value of the zeroth order intensity. For 1a cell, both the zeroth order and the first order intensities are high

indicating that the electrode in this region is periodic with minimal defects. Thus, the Fourier intensities are good indicators of the electrode quality.

4.3 Analysis from microscopic images

4.3.1. Periodicity of HOPG lines

Understanding the importance of periodic structures in device fabrication, a great deal of research is taking place in the development of suitable lithographic techniques. It is highly important to monitor quality of periodic structures produced from various lithographic techniques. The method developed in this work may play a key role in such instances. Here, as an example, a line grating pattern on a Highly Ordered Pyrolytic Graphite (HOPG) fabricated using an ultra-fast laser ablation technique is dealt with [39]. In this technique, a piece of a compact disk (CD) was used as a proximity mask (lithography master). The analysis of both, pattern on CD and HOPG pattern, was undertaken for the sake of comparison.

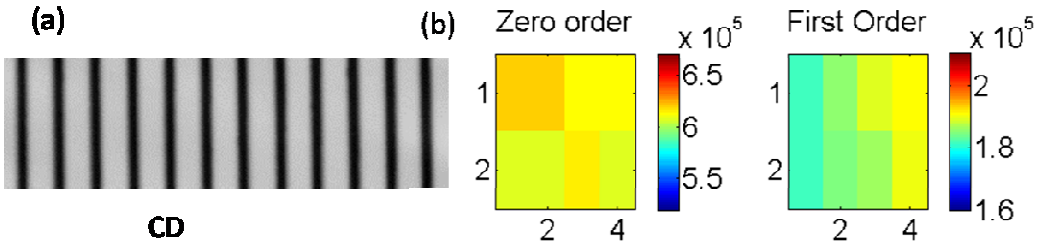

Figure 21. (a) AFM topography of a commercial CD used as master, (b) zeroth order and first order intensities of different cells

Figure 21a shows the AFM topography of a commercially available CD showing periodic lines. It is clear from Figure 18b that the local variations in the zeroth order and the first order intensities are negligible (in second decimal), thus implying that the CD lines are highly periodic.

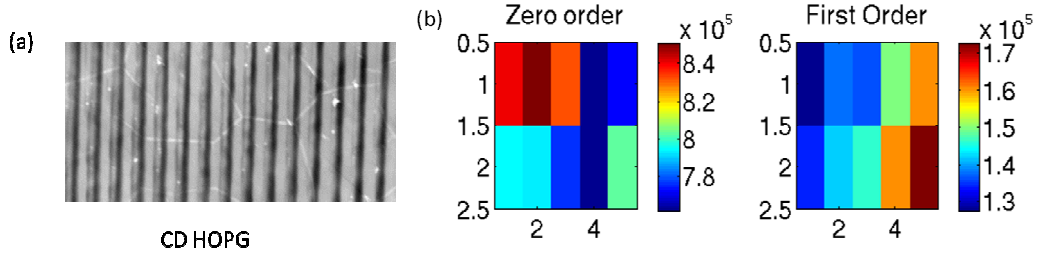

Figure 22. (a) AFM imaging of a grating pattern on HOPG made using CD as mask, (b) zeroth and first order intensities of different cells

Figure 22a shows an HOPG grating fabricated by the laser ablation from CD mask. From the Fourier maps (shown in Figure 22b) it is observed that the first order intensity is not only less compared to that in CD (Figure 21b), the intensity variation among different cells is higher than CD grating. Thus, the periodicity possessed by HOPG is less compare to CD. Brown color in first order intensity represents maximum intensity of first order indicating region with best periodicity while blue color represents minimum value for first order indicating regions with defective periodicity. A similar comparative analysis can be used for any pair of periodic patterns.

4.3.2. Periodicity of biological structures

The concept of studying periodicity is not just limited to computer generated defects or high resolution images. The method can be effectively be applied to literature images by converting them into greyscale BITMAP format demonstrated in **Figure 23**. Figure 23a shows flora genus Selaginella with blue iridescence [1, 40]. Interestingly, the colour possessed by these plants is not any pigment color but a structural colour! If seen in water, it looks green. It is obvious that the plant has evolved to play disguise as a non-green colour would lead to lower photosynthesis efficiency. Rudraksha fruit (*Elaeocarpus angustifolius*) also exhibits blue colour because of the same reason [40]. This laminating structure also acts as antireflective coating for higher wavelengths. Figure

23b shows TEM image of the section of epidermal cells with black lines of cellulose microfibers; Fourier transformation of individual cells (2 × 4 cells) are shown in Figure 23c.

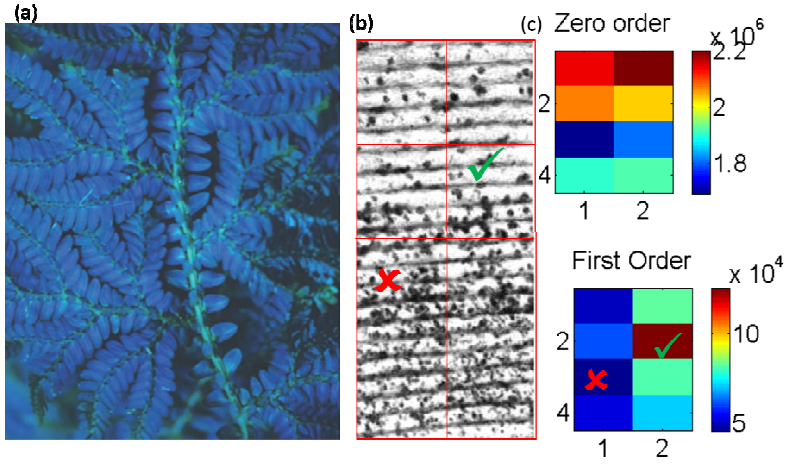

Figure 23. (a) Blue iridescence is exhibited by tropical understory plants of the genus Selaginella. (b) TEM section of a juvenile leaf from the plant Diplaziumtomentosum (c) zeroth order intensity and first order intensity of individual cells (parts). Tick represents a healthy part and cross represents defective part. Image reproduced from [1, 40]

Figure 23c shows that the whole area is not uniformly periodic. If one compares compare the TEM image and the Fourier intensities, one observes that the portions with sharp lines and minimum defects (upper part of TEM image) show maximum first order intensity (brown colour), whereas portions with maximum defects (lower part of TEM image) show minimum first order intensity (blue colour). Thus, method can be used to quantitatively understand periodic structures of biological samples.

4.4 Projected applications in diverse areas

4.4.1. Evaluation of Discipline of Parade

Periodicity is also considered important in National Parades, school assemblies, group dances, chairs positioned in mess/auditorium etc. **Figure 24** shows how difficult it is to evaluate the periodicity of a line.

Figure 24. Drillmaster carefully measuring the length of a stride during the parade
(Photo by Chen Rui)

The method developed in this work is also applicable to simplify this problem. **Figure 25** shows an image of a parade. The parade image was converted into greyscale, divided into 3x1 and then Fourier intensities were obtained; Figure 25b shows the Fourier intensities of individual cells.

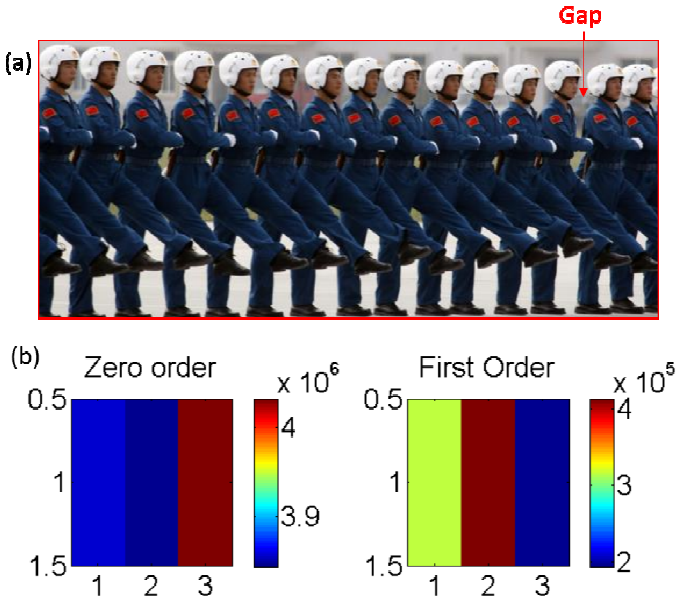

Figure 25. (a) An image of Chinese parade (from: www.newshopper.sulekha.com) (b) zeroth and first order intensity 3x1 map

The first order intensity which is an indicator of periodicity shows a minimum value on the right side and maximum in the centre. Interestingly in the real image, soldiers on the right side do not position themselves uniformly whereas soldiers standing at the centre are at uniform gap. Thus, the first order intensity is able to detect this indiscipline! Hence, the idea can be applied in school assembly and soldier's parades effectively where hundreds of soldiers/ students stand in uniformity and manual check of synchronization of body movement at each command is difficult.

4.4.2. Migration of organisms

The method is not only limited to the materials but periodicity is all around in nature. Thus, it will be useful to bring out all those periodic phenomena. As an example, birds during migration form a special periodic structure (V) to reduce the induced drag by

taking advantages of the air vortices created by the wings of birds flying ahead [41, 42]. The Fourier method can be helpful in understanding the periodic structure of migrating birds of different species in different seasons.

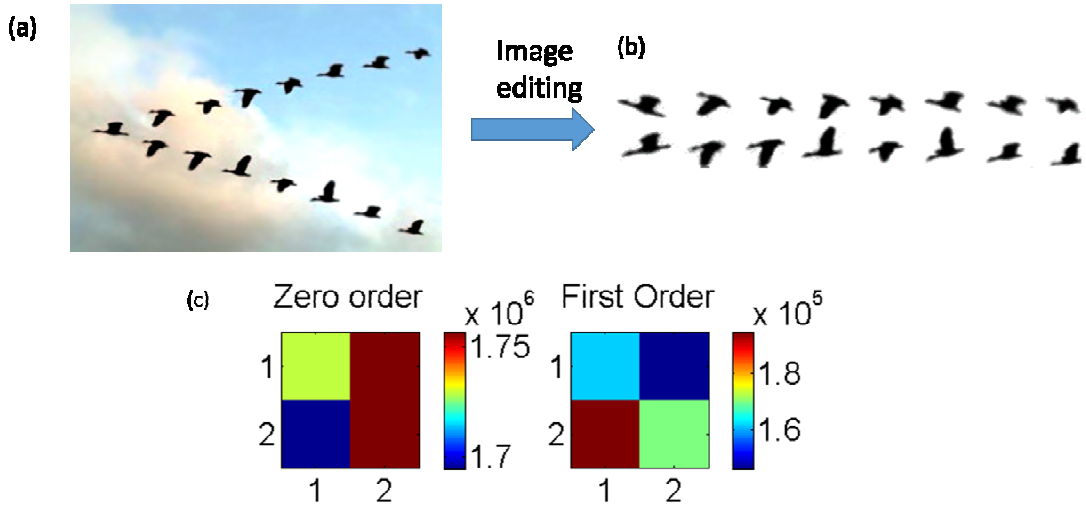

Figure 26. (a) Periodic pattern of birds in sky (from www.wonderwhizkids.com) (b) Edited image with white background (c) zeroth and first order intensity of 2x2 divided pattern

Figure 26a represents some birds forming V shape with nearly equal distance with the bird moving ahead. To perform Fourier transformation, the image is rotated and turned to white background as shown in Figure 26b with Gimp Image Editor Software (Linux OS) required for Fourier mapping. Figure 26c represents the Fourier maps of zeroth order and first order intensities which are in agreement with the periodicity of the real image. The Fourier map can compare the periodicity of birds in different areas. With dynamic images, the method can be applied in evolutionary research to compare migration of various species of organisms showing such behaviour with respect to geographical location and time.

4.4.3. Orographic clouds

Sometimes, clouds also display periodic patterns in sky. **Figure 27** shows a periodic cloud formation known as Orographic wave clouds [43-45]. It is found in moisturized atmosphere above mountains where the cloud forms at cooler crust, while it evaporates at trough due to adiabatic heating. The Fourier method can be useful to study the periodicity of cloud with time.

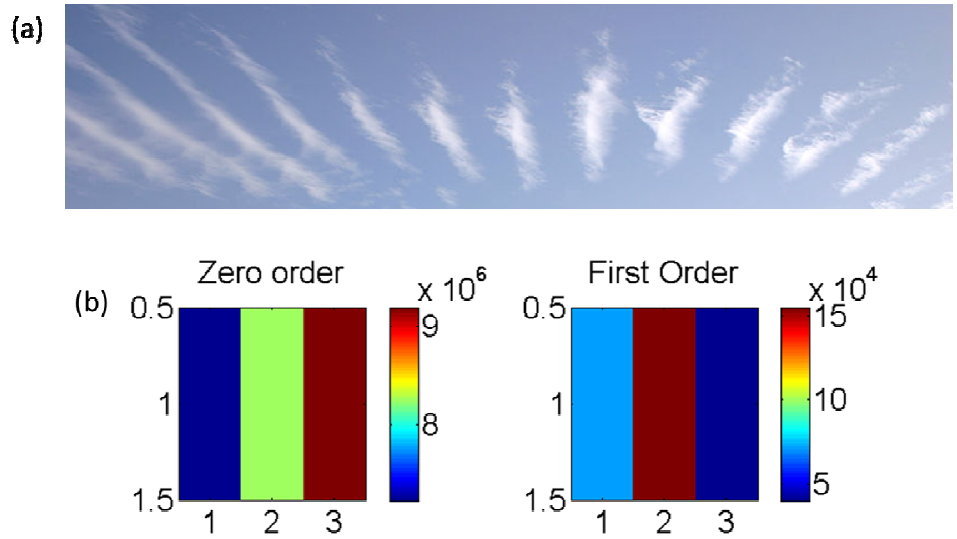

Figure 27. (a) Orographic wavy cloud of Algeria (Wikipedia) (b) zeroth and first order intensity of 3x1 divided image

The idea is demonstrated in **Figure 27** by dividing the image into 3×1 and comparing the first order intensity from them. With dynamical images of clouds and by comparison of the first order intensity with time, the method will be helpful in understanding the mechanism of cloud formation.

4.4.4. Footprints

Foot print of a person is characteristic of his/her mentality and personality. As an example, the handling ability of a cup of coffee depends on walking style of a person [46]. The method can also be applied to study periodicity of footsteps.

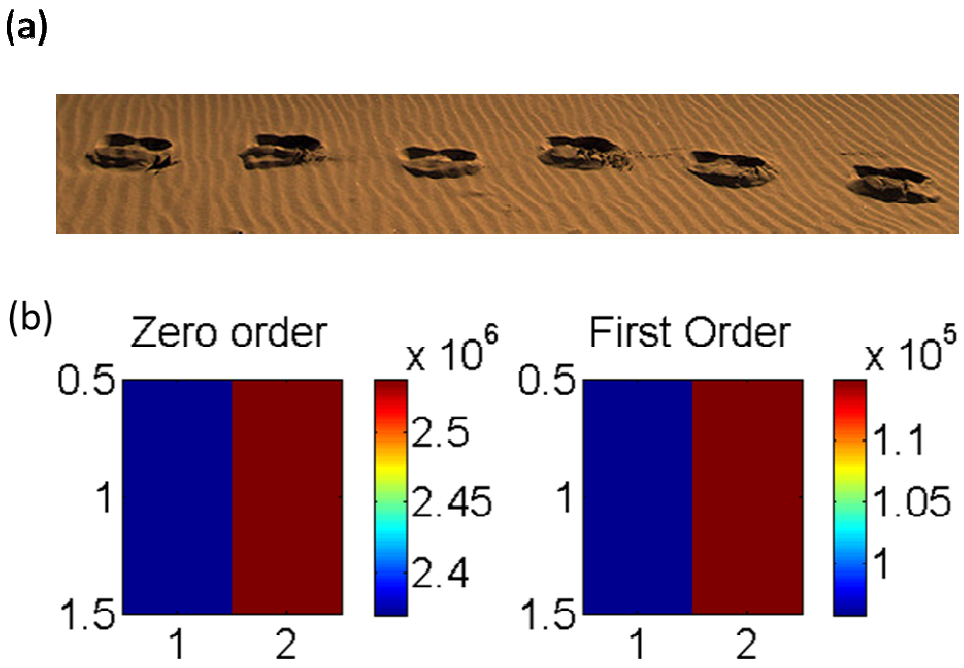

Figure 28. (a) An image of foot prints of a person on sand (from www.flicker.com) (b) zeroth order intensity and first order intensity intesity of 2×1 divided pattern.

Figure 28 shows an image of footprints on sand. The zeroth order and the first order intensities were calculated for 2x1 maps. By using an image of few footsteps, followed by calculation of first order intensity and its standard deviation, one can understand stability and uniformity of the walk. Higher value of the first order intensity and lesser value of the standard deviation indicate periodic and stable motion. Psychologists may use this method to compare foot prints of persons in different moods for instance, walking style of drunkard person etc.

5. Conclusion:

A general method to identify and quantify defects is proposed; aperiodicity and non-uniformity of any surface may be analysed based on the image contrast between the defect and the periodic structure, the periodicity may be inherent to the surface else superimposed. The method relies on Fourier transformation. The Fourier intensities were first analysed for computer generated images with respect to size, shape, and position of the defect in periodic gratings. The analysis showed that the zeroth order intensity is sensitive only to the size of the defects whereas the first order intensity is sensitive to shape and position also. Thus, the first order intensity gives information far better than the zeroth order. Zeroth order intensity and the fill factor are particularly not sensitive if multiple types of defects are present in the sample, whereas the first order is highly effective to detect minute differences. When using an external overlaid grating its positioning can also change the Fourier intensities as the grating can cover the defects in different ways. To tackle this problem, taking the mean of Fourier maps of overlapped images produced with various grating phases, is proposed and successfully demonstrated by taking the example of circle defects.

An experimental prototype of the idea is demonstrated by overlaying a grating on defects represented by beads. Relative variation in the Fourier intensities showed a proportionality relation with the number of beads in the area thus, opening up scope to study unknown defects with Fourier intensities.

The Fourier method may play important role in various applications. Many such instances have been dealt within the thesis. The computer code can be customized for specific applications.

Periodic structure are central to photonic crystals, meta-materials, sensors, waveguides, memory arrays , transparent electrodes, DNA chips etc. These are fabricated by a variety of methods- chemical and physical routes, self assembly and multi-lithographic steps where monitoring of the uniformity of the resulting structure is highly desirable. The Fourier method developed in this study will be very useful in the evaluation of such structures. It is particularly useful in quality monitoring of industrial products.

Dynamics and kinetics of self- assembly can be effectively studied by taking in situ optical imaging of colloids/ beads undergoing self-assembly. By studying the Fourier intensities with respect to time, kinetics of self assembly can be quantitatively studied.

It is very difficult to monitor uniform and synchronized steps in national parades, school parades where hundreds of soldiers/ students parade on same command. The Fourier method developed in the study can perform this monitoring in a matter of seconds. The Fourier method may be supportive in understanding synchronization of steps among dance performers similar to Parade. This Fourier method can be extended to evaluate any interesting ordered object including chairs in big auditorium/mess and cars in parking. A slight wrong position in the arrangement will show its signature in the first order intensity thus, large scale ordered arrangement can be monitored easily.

Currently it is very difficult to compare printers or scanners; which generally claim similar specifications in terms of dpi. The Fourier method can be helpful in comparison of their real scanned /printed outcomes. Images obtained by scanning an ideal grating can be scanned in different scanners and comparison can be done by the Fourier intensities and corresponding standard deviations; with Fourier maps, one can even locate the defective area of the scanner bed.

Research related to migration of birds, oliographic wave clouds, sea waves and footprints etc. can also be aided by doing dynamical Fourier intensity studies (studying Fourier intensities with respect to time). Thus the present study has wider scope in diverse areas.

6. References

1. Vukusic, P. & Sambles, J. R. Photonic structures in biology. *Nature* **424**, 852-855 (2003).
2. Kinoshita, S., Yoshioka, S. & Miyazaki, J. Physics of structural colors. *Reports on Progress in Physics* **71**, 076401 (2008).
3. Kinoshita, S. & Yoshioka, S. Structural Colors in Nature: The Role of Regularity and Irregularity in the Structure. *ChemPhysChem* **6**, 1442-1459 (2005).
4. Elachi, C. Waves in active and passive periodic structures: A review. *Proceedings of the IEEE* **64**, 1666-1698 (1976).
5. Gantzounis, G., Stefanou, N. & Papanikolaou, N. Optical properties of periodic structures of metallic nanodisks. *Physical Review B* **77**, 035101 (2008).
6. Sibilia, C. *et al.* Electromagnetic properties of periodic and quasi-periodic one-dimensional, metallo-dielectric photonic band gap structures. *Journal of Optics A: Pure and Applied Optics* **1**, 490 (1999).
7. Tabatadze, V., Petoev, I. & Zaridze, R. in *Direct and Inverse Problems of Electromagnetic and Acoustic Wave Theory (DIPED), 2010 Xvth International Seminar/Workshop on.* 50-53.
8. Gupta, R., Sagade, A. A. & Kulkarni, G. U. A low cost optical hydrogen sensing device using nanocrystalline Pd grating. *International Journal of Hydrogen Energy* **37**, 9443-9449 (2012).
9. Nozar, P., Dionigi, C., Migliori, A., Calestani, G. & Cademartiri, L. The early stages of the self-assembly process of polystyrene beads for photonic applications. *Synthetic Metals* **139**, 667-670 (2003).

10. Sharp, D. N. *et al.* Photonic crystals for the visible spectrum by holographic lithography. *Optical and Quantum Electronics* **34**, 3-12 (2002).

11. Li, J., Fattal, D. & Li, Z. Plasmonic optical antennas on dielectric gratings with high field enhancement for surface enhanced Raman spectroscopy. *Applied Physics Letters* **94**, 263114-263113 (2009).

12. Im, S. H. *et al.* Synthesis of polystyrene beads loaded with dual luminophors for self-referenced oxygen sensing. *Talanta* **67**, 492-497 (2005).

13. McCarty, L. S., Winkleman, A. & Whitesides, G. M. Electrostatic Self-Assembly of Polystyrene Microspheres by Using Chemically Directed Contact Electrification. *Angewandte Chemie International Edition* **46**, 206-209 (2007).

14. Tan, B. J. Y. *et al.* Fabrication of a Two-Dimensional Periodic Non-Close-Packed Array of Polystyrene Particles. *The Journal of Physical Chemistry B* **108**, 18575-18579 (2004).

15. Wu, S.-K., Tang, T.-P. & Tseng, W. Self-assembly of polystyrene microspheres within spatially confined rectangular microgrooves. *J Mater Sci* **43**, 6453-6458 (2008).

16. Karp, J. H., Tremblay, E. J. & Ford, J. E. Planar micro-optic solar concentrator. *Opt. Express* **18**, 1122-1133 (2010).

17. Hye Jin, N. *et al.* in *Optoelectronic and Microelectronic Materials and Devices, 2008. COMMAD 2008. Conference on.* 246-248.

18. Tseng, J. K., Chen, Y. J., Pan, C. T., Wu, T. T. & Chung, M. H. Application of optical film with micro-lens array on a solar concentrator. *Solar Energy* **85**, 2167-2178 (2011).

19. Hook, A. L., Voelcker, N. H. & Thissen, H. Patterned and switchable surfaces for biomolecular manipulation. *Acta Biomaterialia* **5**, 2350-2370 (2009).

20. Pirrung, M. C. How to Make a DNA Chip. *Angewandte Chemie International Edition* **41**, 1276-1289 (2002).

21. Brown, P. O. & Botstein, D. Exploring the new world of the genome with DNA microarrays. *Nat Genet*.

22. Whitesides, G. M. & Grzybowski, B. Self-Assembly at All Scales. *Science* **295**, 2418-2421 (2002).

23. Yin, Y. & Xia, Y. Self-Assembly of Monodispersed Spherical Colloids into Complex Aggregates with Well-Defined Sizes, Shapes, and Structures. *Advanced Materials* **13**, 267-271 (2001).

24. Pacholski, C., Kornowski, A. & Weller, H. Self-Assembly of ZnO: From Nanodots to Nanorods. *Angewandte Chemie International Edition* **41**, 1188-1191 (2002).

25. Arecchi, F. T., Bertani, D. & Ciliberto, S. A fast versatile optical profilometer. *Optics Communications* **31**, 263-266 (1979).

26. Tang, S. & Hung, Y. Y. Fast profilometer for the automatic measurement of 3-D object shapes. *Appl. Opt.* **29**, 3012-3018 (1990).

27. Whitefield, R. J. Noncontact optical profilometer. *Appl. Opt.* **14**, 2480-2485 (1975).

28. Shimizu, Ibarki I. Method and Apparatues for Image Inspection. US patent US 2007/0230819 A1 (2007).

29. Nolte, D.L. *et al.* Laser scanning interferometric surface metrology. US patent US 7405831 (2008).

30. David, Treves *et al.* Method and apparatus for inspecting substrates. US patent US 6548821 (2003).

31. Benjamin, J. Pernick *et.al.* Optical surface roughness detection method and apparatus. US patent US 4334780 (1982).

32. Blasius, Brezoczky *et al* Surface inspection of a disk by diffraction pattern sampling. US patent US 5781649 (1998).

33. Meeks, S *et al.* System and method for double sided optical inspection of thin film disks or wafers. US patent US 7061601 (2006).

34. Gupta, R. & Kulkarni, G. U. Holistic Method for Evaluating Large Area Transparent Conducting Electrodes. *ACS Applied Materials & Interfaces* **5**, 730-736 (2012).

35. Van Loan, C., Industrial, S. f. & Mathematics, A. *Computational Frameworks for the Fast Fourier Transform*. (Society for Industrial and Applied Mathematics, 1992).

36. Zuazo, J. D. *Fourier Analysis*. (American Math. Soc., 2001).

37. Cooley, J. W. & Tukey, J. W. {An algorithm for the machine calculation of complex Fourier series}. *Mathematics of computation* **19**, 297-301 (1965).

38. Lee, J. *et al.* Very long Ag nanowire synthesis and its application in a highly transparent, conductive and flexible metal electrode touch panel. *Nanoscale* **4**, 6408-6414 (2012).

39. Kurra, N., Sagade, A. A. & Kulkarni, G. U. Ultrafast Direct Ablative Patterning of HOPG by Single Laser Pulses to Produce Graphene Ribbons. *Advanced Functional Materials* **21**, 3836-3842 (2011).

40. Lee, D. W. Iridescent blue plants. *American Scientist* **85**, 56-63 (1997).

41. Berthold, P. *Bird Migration: A General Survey*. (Oxford University Press, 2001).

42. Lincoln, F. C., Anatasi, P. A., Peterson, S. R., Zimmerman, J. L. & Hines, B. *Migration of Birds*. (U.S. Government Printing Office, 1999).

43. Garrett, A. J. Orographic cloud over the eastern slopes of Mauna Loa volcano, Hawaii, related to insolation and wind *Mon. Weather Rev***108** 931-941 (1980).

44. Martinsson, B. G. *et al.* Droplet nucleation and growth in orographic clouds in relation to the aerosol population. *Atmospheric Research* **50**, 289-315 (1999).

45. Lynn, B., Khain, A., Rosenfeld, D. & Woodley, W. L. Effects of aerosols on precipitation from orographic clouds. *Journal of Geophysical Research: Atmospheres* **112**, D10225 (2007).

46. Mayer, H. C. & Krechetnikov, R. Walking with coffee: Why does it spill? *Physical Review E* **85** (2012).